# On the Feasibility of the Visible Wavelength, At-A-Distance and On-The-Move Iris Recognition

*(Invited Paper)*

Hugo Proença

***Abstract*— The dramatic growth in practical applications for iris biometrics has been accompanied by relevant developments in the underlying algorithms and techniques. Among others, one active research area concerns about the development of iris recognition systems less constrained to users, either increasing the imaging distances, simplifying the acquisition protocols or the required lighting conditions. In this paper we address the possibility of perform reliable recognition using visible wavelength images captured under high heterogeneous lighting conditions, with subjects at-a-distance (between 4 and 8 meters) and on-the-move. The feasibility of this extremely ambitious type of recognition is analyzed, its major obstacles and challenges discussed and some directions for forthcoming work pointed.**

## I. Introduction

BEing an internal organ, naturally protected, visible from the exterior and supporting contactless data acquisition, the human iris has - together with the face - the potential of being imaged covertly. Additionally, its almost circular and planar shape turns the iris region easier to parameterize, in order to compensate for angular deviations resultant from off-angle image capturing. These properties leaded to the ambition of move one step ahead and perform covert iris recognition, which remains to be achieved. Clearly, this type of recognition systems will broad the biometrics applicability to scenarios where the subjects' cooperation is not expected, which has evident interesting security and forensic applications (e.g., criminal/terrorist seek and missing children). This area motivates growing interests on the research community and constituted the scope of a large number of recent publications (e.g., [1], [2] and [3]).

Currently deployed iris recognition systems rely on good quality images, captured in a stop-and-stare interface, at close distances and near infrared wavelengths (NIR, 700-900 nm). The use of active NIR lighting sources enables the utilization of imaging filters that block the wavelengths outside the desired interval, whose are usually correspondent to reflections that occlude portions of the iris texture (figure 1). Also, these systems require high illumination levels, sufficient to maximize signal/noise ratio in sensor and to capture sufficient contrast of the iris features. However, the safety limit of illumination - defined at about 10 mw / $cm^2$ by both American and European standards counsel boards ([4] and [5]) - must be taken into account, at it is known that too high illumination levels cause permanent eye damage. Here, the NIR wavelength is particularly hazardous because the eye does not instinctively respond with its natural mechanisms (aversion, blinking and pupil contraction).

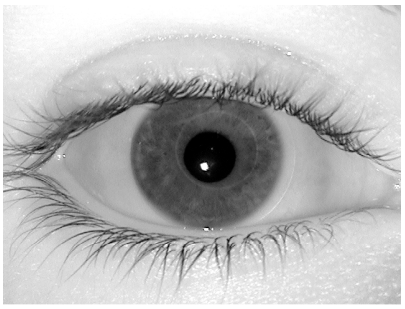

*(a) Near infra-red image, acquired under high constrained conditions (WVU database [6]).*

*(b) Visible wavelength image, acquired at-a-distance and on-the-move (UBIRIS.v2 database [7]).*

Fig. 1. Illustration of the typical differences between close-up iris images acquired on high constrained conditions in the near infra-red wavelength (figure 1a) and images acquired in the visible wavelength, on less constrained imaging conditions (figure 1b).

If NIR wavelengths were used in the acquisition of at-a-distance iris images, acceptable depth-of-field values would demand significantly higher f-numbers on the optical system, which will have (squared) direct correspondence with the amount of light required to the process. Also, the motion factor will demand very short exposure times, whose again will imply higher levels of light. Due to the aforementioned safety reasons, the process feasibility using NIR light is strongly conditioned.

According to this discussion, the feasibility of at-a-

Hugo Proença is with the Department of Computer Science, at the University of Beira Interior, Covilhã, Portugal (email: hugomcp@di.ubi.pt).

This work was supported by "FCT-Fundação para a Ciência e Tecnologia" and "FEDER" in the scope of the PTDC/EIA/69106/2006 research project "BIOREC: Non-Cooperative Biometric Recognition".

distance and on-the-move iris recognition is constrained to the use of visible wavelength light. However, should it be possible to perform this type of recognition? What challenges arise from unconstrained imaging environments? Is it realistic to expect reliable recognition on this scenario?

As before stated, several issues remain to achieve deployable covert iris recognition systems. Unquestionably, these type of systems will constitute a tradeoff between the quality of the captured data and the recognition accuracy.

In this paper, we address the feasibility of this extremely ambitious type of biometric recognition from three different perspectives:

- Amount of information. This focuses on the amount of information that - on average - is possible to capture on the described conditions. Using an imaging framework described on section II-A and without requiring subjects' cooperation, how much discriminant information is captured? How does it varies, regarding the image acquisition distance? Do the levels of iris pigmentation strongly constraint the imaging process, as pointed on previous works (e.g., [8])? In this analysis we used a statistical measure of randomness widely used to characterize textures: the image entropy.
- Specificity. The role of the specificity achieved by the discussed recognition systems should be emphasized. Due to the unconstrained and high dynamic imaging conditions, the capturing of poor quality data is high probable. In order to increase the confidence on any positive recognition, it should be granted that these type of systems will not frequently produce false acceptances, namely when matching extremely degraded data. Here, we followed the classical Daugman's recognition approach ([9], [10] and [11]) to perform iris segmentation, encoding and matching.
- Sensitivity. Finally we estimated the probability for the occurrence of false non-matches on these type of systems. Again, we used the Daugman's recognition approach to encode and compare signatures extracted from a set of good quality images (used as templates) and a set of degraded samples.

The rest of this paper is organized as follows: Section II discusses the imaging framework and protocol used in our experiments, as well illustrates the resultant non-ideal images. Section III describes our experiments, focusing on the amount of captured information and on the sensitivity and specificity that recognition systems would achieve on these circumstances. Finally, Section IV concludes the paper and points directions for further work.

## II. Visible Wavelength Iris Images

In this section we describe the most relevant parameters of an imaging framework that operates on the visible wavelength and is able to capture close-up iris images from at-a-distance and on-the-move subjects. It should be mentioned that although all the images illustrated in this paper were captured and cropped manually, we are currently finishing a prototype of an imaging framework that completely automates the close-up iris imaging procedure.

### *A. At-A-Distance and On-The-Move Image Capturing*

| **Image Acquisition Framework and Set-Up** | |
|---|---|
| Camera = Canon EOS 5D | Color Representation = sRGB |
| Shutter Speed = 1/197 sec. | Lens Aperture = F/6.4 - F/7 |
| Focal Length = 400 mm | F-Number = F/6.3 - F/7.1 |
| Exposure Time = 1/200 sec. | ISO Speed = ISO-1600 |
| Metering Mode = Pattern | |
| **Details of the Resultant Close-Up Iris Images** | |
| Width = 800 pixels | Height = 600 pixels |
| Format = tiff | Bit Depth = 24 bit |
| Horizontal Resolution = 72 dpi | Vertical Resolution = 72 dpi |

TABLE I
DETAILS OF THE IMAGE ACQUISITION FRAMEWORK AND SETUP, AS WELL OF THE RESULTANT IMAGES.

Table I details the setup of the imaging framework used in our experiments and the main characteristics of the resultant images. This framework was installed on a lounge under natural light and with varying sources of artificial visible light. We placed several marks on the floor (between three and ten meters away from the acquisition camera) and acquired images from moving subjects (figure 2). This process leaded to the appearance of a large number of non-ideal images, with several regions of the iris rings occluded by reflections, as well significant iris obstructions due to eyelids and eyelashes.

### *B. Non-Ideal Images*

Fig. 3. Examples of close-up iris images acquired at varying distances (between four and eight meters), at the visible wavelength, from on-the-move subjects and under high dynamic lighting conditions.

As it is expected from the afore described imaging conditions, it is high probable that the captured data has heterogeneous quality and multiple noise factors. Through visual inspection, we identified fourteen different types of these, classified into *local* or *global* as they affect image regions or the complete image. The *local* category comprises iris occlusions due to eyelids, eyelashes, glasses, reflections,

(a) *Eight meters.* (b) *Seven meters.* (c) *Six meters.* (d) *Five meters.* (e) *Four meters.*

Fig. 2. Sequence of close-up iris images acquired at the visible wavelength, from between eight (figure 2a) and four (figure 2e) meters on a continuously moving subject, under dynamic lighting conditions and without requiring to the user any type of cooperation.

off-angle and partial images, and the *global* comprises poor focused, motion-blurred, rotated, improper lighting and out-of-iris images. Figure 3 illustrates some of the types of non-ideal images that result of the imaging conditions and protocol focused on this paper.

## III. Experiments

In this section we detail the performed experiments, describe the used data sets and discuss the corresponding results.

### A. Amount of Captured Information

As stated above, our initial analysis focused on the amount of information contained on the regions correspondent to the iris, regarding the distance from where images were captured. We divided the initial set of 1 000 images into five subsets, each one including images respectively captured from distances of 4, 5, 6, 7 and 8 meters. Further, anticipating that the levels of iris pigmentation should play an important role, we sub-divided the images into three categories, according to this criterium: 'light" category contains the blue and light green irises, "medium" contains the light and medium brown and the dark green irises and, finally, "heavy' contains the dark brown and almost black irises.

The upper-right region of figure 4 illustrates the performed experiments. We started by the segmentation of each iris region, localized its noisy regions and normalized it into a dimensionless polar coordinate system, through a process known as the "Daugman Rubber Sheet".

It is known the most successful iris encoding methods operate locally, i.e., each signature component is extracted from a small iris region (e.g., Daugman's encoding strategy iteratively convolves pairs of Gabor kernels along regions of the normalized iris data), which leaded us to measure the amount of information locally, on $7 \times 7$ windows of the normalized images. This gives an idea about the amount of information available on each region from where the components of the signature are extracted.

Image entropy has been widely used in the image processing domain to characterize textures, as a measure of the amount of information contained by an image. It is defined as

$$h(I) = -\sum_{0}^{g-1} p(k)\ log_2(p(k)) \qquad (1)$$

where $I$ is an image with $g$ gray levels, and $p(k)$ is the probability of occurrence of the gray level $k$ in $I$.

Figure 4 illustrates the local entropy values obtained for the "light" pigmented irises in our experiments. For each imaging distance, the upper plot assess whether values could come from a Gaussian distribution (normal data will appear linear). The corresponding lower plot gives the histogram and the fitted Gaussian distribution with parameters shown in the plot's corner. "R-square" gives the goodness-of-fit of the data to the corresponding Gaussian distribution.

We observed that, either for "light", "medium" and "heavy" pigmented irises, values almost perfectly fit Gaussian distributions, as the R-square values were all above 0.96 (1 corresponds to a perfect Gaussian distribution). Also, we confirmed that the average entropy values have inverse correspondence with the imaging distance and with the levels of iris pigmentation. This is summarized in figure 5. The $X$ and $Y$ axes respectively give the imaging distance and the levels of iris pigmentation. The vertical axis gives the average local entropy values within the normalized iris regions.

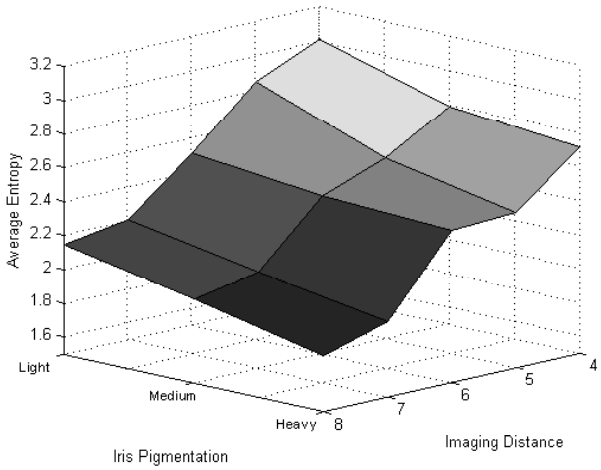


Fig. 5. Impact of the image acquisition distance and of the levels of iris pigmentation on the amount of information captured with the afore described image acquisition framework and protocol. The vertical axis gives the average of the entropy values on $7 \times 7$ windows located within the normalized iris rings. For comparison purposes it should be mentioned that a corresponding value of $3.68$ was obtained for images acquired in the NIR wavelength and on cooperative scenarios.

Apart the confirmation of the relationship between the

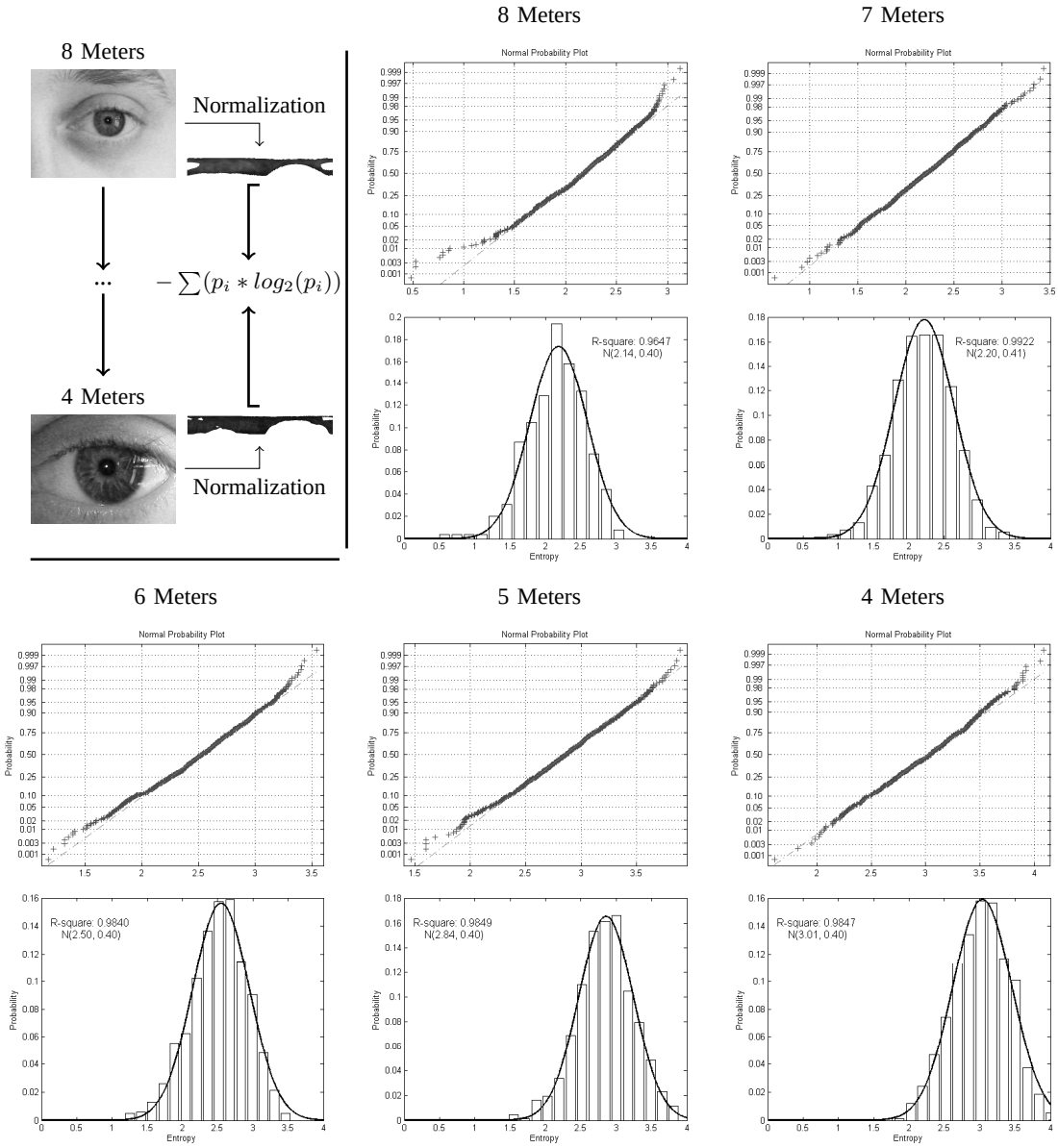


Fig. 4. Measuring of the average entropy of 7 $\times$ 7 windows located within the iris rings, regarding the image acquisition distance. As illustrated in the upper left corner, we segmented and normalized a set of close-up iris images and analyzed the amount of information that is possible to capture in these situations. The upper sub-figure of each column gives the spread of the values along an optimal Gaussian distribution plotted linearly. The lower sub-figure gives the correspondent histogram, the approximated Gaussian parameters and a goodness-of-fit measure (R-square).

amount of captured information, the imaging distance and the levels of iris pigmentation, these experiments allowed us to perceive *how much* values decrease and to obtain lower bound values for the recognition feasibility. As comparison term, in figure 6 we show the correspondent results obtained for an image of the WVU [6] database. This image was acquired in a stop-and-stare interface, at close distances and near infrared (700-900 nm.) wavelengths, corresponding to the acquisition conditions and protocols used in successfully deployed iris recognition systems. The similarity between the distribution of the values obtained on images acquired in the cooperative scenario and ours is evident, although a comprehensible gap in the average value can be observed. We concluded that images captured from 8, 7, 6, 5 and 4 meters have respectively 58, 59, 67, 77 and 81% of the amount of information available on the regions of a good quality IR image, acquired in a cooperative scenario. Forthcoming work is required to analyze the relationship between the recognition error rates and this information gap.

### *B. Specificity*

Several previous works about the iris recognition technology reported a very small - almost infinitesimal - probability of produce a false match in the comparison between signatures extracted from data with good quality

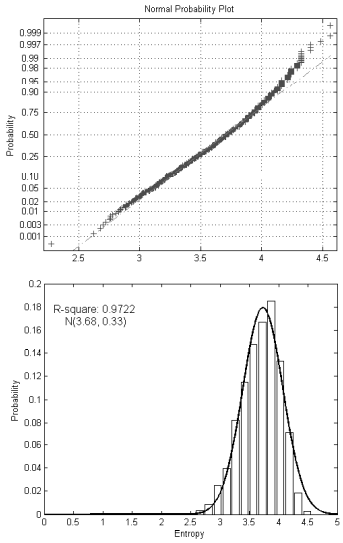


Fig. 6. The upper figure gives the distribution of the entropy values of $7 \times 7$ windows located within the iris ring of the infra-red image shown in figure 1a, acquired in a stop-and-stare interface, at close distance and requiring the subject's cooperation. This type of image represents the image acquisition conditions of already deployed iris recognition systems. On the bottom figure, the respective histogram is given. "R-square" corresponds to the goodness-of-fit of the plotted Gaussian distribution with $\mu = 3.68$ and $\sigma = 0.33$ to the obtained results.

(e.g., [10], [12], [13] and [14]). This is due to the chaotic appearance of the iris texture's main components and is regarded as one of the technology's major advantages, when compared with other biometric traits. However, a fundamental hypothesis for the feasibility of the type of recognition discussed in this paper should be tested: to assure that the comparison between signature templates (extracted from iris data with good quality) and samples extracted from iris data with very poor quality or even from partial or non-iris regions (due to failures on the eye detection and segmentation modules, high probable in high dynamic environments) will neither frequently produce false matches, whose would take most of the value given to any reported positive recognition.

This hypothesis was tested through a procedure illustrated in figure 7. Using the recognition method proposed by Daugman [15] - composed by iris segmentation, normalization (Daugman Rubber Sheet), encoding (bidimensional Gabor wavelets) and matching (Hamming distance) - we extracted 1 000 signatures from iris images with good quality and recorded them in a templates database. Further, we built a set of sample signatures, extracted from 1 000 iris images with very poor quality, 10 000 non-iris or partial iris images and 10 000 natural and synthetic textures images. Finally, we performed a "1-to-all" comparison, between each sample and the set of templates, giving a total of 21 000 000 comparisons. During these tests we didn't get a single dissimilarity value close to the usual acceptance threshold (0.33) and, thus, not even a single false acceptance was observed.

Figure 8 gives the histogram of the obtained dissimilarity values (vertical bars) and the approximated Gaussian distribution (line plot with $\mu = 0.49992$ and $\sigma = 0.02419$). We confirmed that, even on high degraded data, the used iris encoding and comparison strategies produce a false match with almost null probability. Based on the parameters of the fitted Gaussian distribution, the probability of producing a dissimilarity value lower than 0.33 will be approximately of $1.03923 \times 10^{-12}$. Once again, the role of this value for the type of recognition discussed in this paper should be stressed: it can be assumed with extreme high confidence that such recognition systems will not produce false matches and, thus, any match reported has a full probability of being genuine. This means that, independently of the false non-matches' frequency (due to extreme lighting variations, movements and perspectives) any positive recognition is high reliable and should be regarded as a gain, as it cames from completely human-free efforts process.

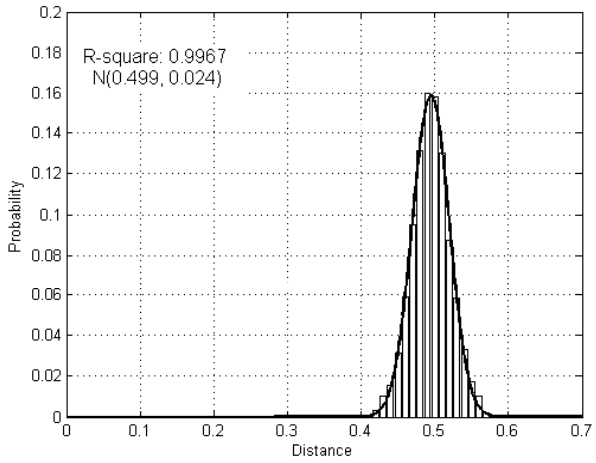


Fig. 8. Histogram of the obtained dissimilarities when comparing signatures extracted from 1 000 templates with good quality and 21 000 signatures extracted from iris images with bad quality, partial irises and non-iris data. "R-square" gives the goodness-of-fit of the plotted Gaussian distribution with $\mu = 0.499$ and $\sigma = 0.024$ to the obtained results.

### *C. Sensitivity*

As stated before, several authors reported the levels of iris pigmentation as a strong obstacle to its proper visible wavelength imaging. It is considered that heavy pigmented irises, that constitute the large majority of the world population, would demand strong amounts of light to be acquired with sufficient discriminating information. Here, we infer *how much* the levels of iris pigmentation increase the recognition challenges. This was made through an analysis of the separability between the intra- and inter-class comparisons regarding the levels of iris pigmentation, which gives an approximation for the sensitivity that recognition systems achieve on the correspondent type of irises. Once again, we divided the available images into three sub-sets: "light", "medium" and "heavy" pigmented irises, each one with varying imaging distances and image quality. Then, we performed every possible intra- and inter-class comparison,

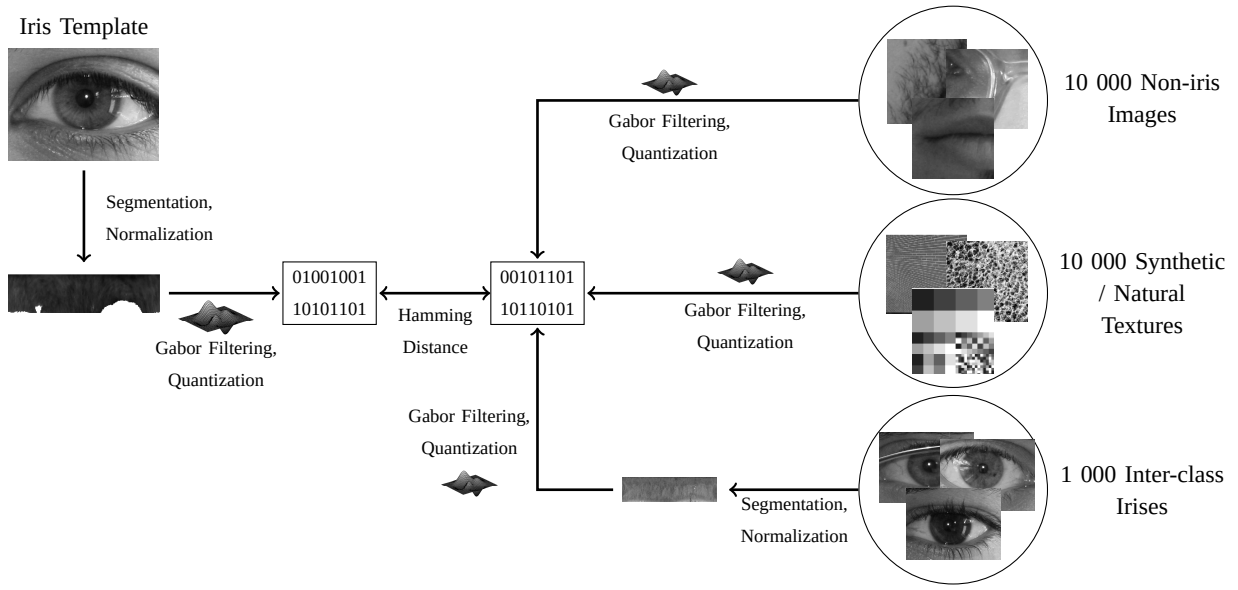


Fig. 7. Setup of the experiments performed to evaluate the probability of produce a false match in the comparison between iris signatures extracted from good quality data ("iris template") and signature samples resultant from iris data with bad quality, or even partial or non-iris data. We used the main recognition stages proposed by Daugman and successfully deployed in recognition systems to evaluate the probability of produce a false match in these situations.

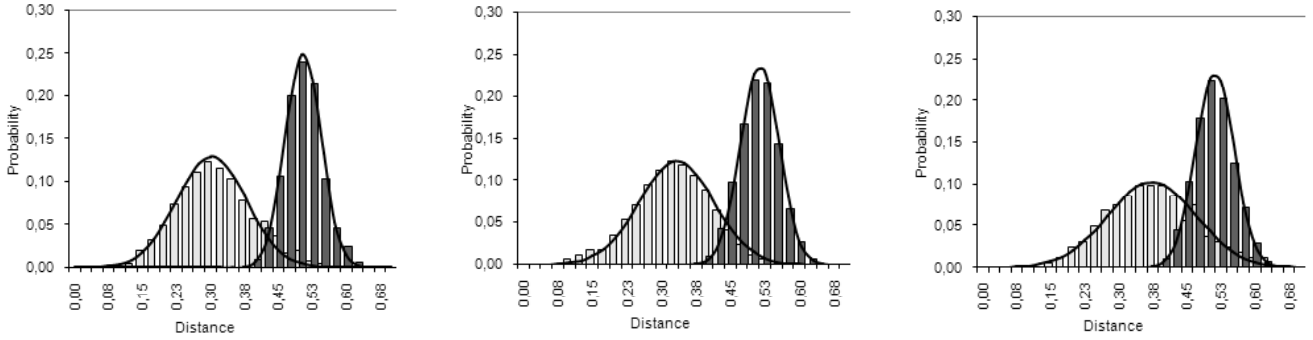


*(a)* *'Light' irises,* $\mu_I = 0.29$, $\sigma_I = 0.07$, $\mu_E = 0.49$, $\sigma_E = 0.03$, $\tau = 2.350$

*(b)* *'Medium' irises,* $\mu_I = 0.32$, $\sigma_I = 0.08$, $\mu_E = 0.50$, $\sigma_E = 0.04$, $\tau = 1.994$

*(c)* *'Heavy' irises,* $\mu_I = 0.36$, $\sigma_I = 0.09$, $\mu_E = 0.49$, $\sigma_E = 0.04$, $\tau = 1.317$

Fig. 9. Separability between intra- and inter-class comparisons, regarding the levels of iris pigmentation. The light and dark bar series represent respectively the intra- and inter-class comparisons and the dotted line series fitted Gaussian distributions. $\tau$ gives the value of the Fisher-ratio test (2).

from which the recognition decidability [16] was measured and the system's feasibility inferred.

Figure 9 contains the three obtained histograms, respectively for "light" (figure 9a), "medium" (figure 9b) and "heavy" (figure 9c) pigmented irises. $\tau$ gives a Fisher-ratio test indicator of the system's decidability:

$$\tau = \frac{\mu_E - \mu_I}{\sqrt{\frac{1}{2}(\sigma_E^2 + \sigma_I^2)}} \tag{2}$$

where $\mu_I$ and $\mu_E$ denote the intra- and inter-class mean values and $\sigma_I$ and $\sigma_E$ the respective standard deviation values.

At first, we observed that the parameters obtained for the inter-class comparisons were approximately equal for all types of irises, which confirms the results given in the last section. Also, an evident decrease in the separability between intra- and inter- class comparisons regarding the levels of iris pigmentation was observed, as the values of $\tau$ summarize. Without surprise we obtained decidability values that are far from the values that traditionally are accepted as good (above 3.0 [16]). This can be easily justified by the extreme poor data quality and the dynamics of the environment from where data was acquired.

On the other hand, it should be stressed that obtained values are - clearly - not chaotic, and an evident discrimination between intra- and inter- class comparisons can be

observed for all types of irises. Thus, it can be concluded that, although with relatively low sensitivity values, it is possible to recognize individuals using visible wavelength images, even on high pigmented irises. Once again, we stress that this conclusion results from the fact that the whole recognition process is completely free of any human effort. It is obvious that even close values obtained on cooperative scenarios will make this type of systems clearly impracticable.

If the *standard* dissimilarity value of 0.33 is used to accept a match between signatures, 81%, 65% and 43% of the intra-class comparisons respectively for "light", "medium" and "heavy" pigmented irises are below that limit. This gives an approximation about the potential sensitivity achieved for the correspondent levels of iris pigmentation, which from our viewpoint constitutes an encouragement for further research on the area and stresses the recognition feasibility.

## IV. Conclusions

All the successfully deployed iris recognition systems use NIR active light sources to acquire images at very limited distances and demand users a strong cooperative behavior, which denies the broadening of the technology to areas where the subjects cooperation is not expectable (e.g., terrorist/criminal seek, missing children).

Clearly, the use of NIR light to acquire images at larger distances would demand stronger lighter sources, whose are particularly hazardous to subjects' health due to the nonexistence of eye's natural protective mechanisms (aversion, blinking and pupil contraction). One alternative is the performing of visible wavelength at-a-distance and on-the-move image capturing, minimizing the probability of risk to subjects eyes.

In this paper a set of images of the UBIRIS.v2 database - captured on the afore described conditions - was used to give some results about the amount of information that is possible to capture, the probability to produce false acceptances and the maximal sensitivity that recognition systems should achieve in these extremely ambitious scenarios. The experiments led us to confirm the increasing difficulty of proper imaging and recognition on heavy pigmented irises. Also, we observed the practical null probability of produce false matches (even when using high degraded data) and obtained rough approximations for the sensitivity and specificity that the type of recognition systems discussed in this paper could obtain.

Finally, it should be stressed that all the results given in this paper were obtained when using iris segmentation, encoding and matching methods though to cooperative and NIR wavelength scenarios. The development of alternate and specialized techniques able to deal with the intrinsic properties of the focused environments should significantly improve the results, which we believe to encourage further research on the area.

## Acknowledgments

We acknowledge the financial support given by "FCT-Fundação para a Ciência e Tecnologia" and "FEDER" in the scope of the PTDC/EIA/69106/2006 research project "BIOREC: Non-Cooperative Biometric Recognition".

## References

[1] H. Proença and L. A. Alexandre, "Toward non-cooperative iris recognition: A classification approach using multiple signatures," *IEEE Transactions on Pattern Analysis and Machine Inteligence, vol. 9, no.4*, pp. 607–612, 2007.

[2] N. S. N. B. Puhan and X. Jiang, "Robust eyeball segmentation in noisy iris images using fourier spectral density," in *Proceeding of the* $6^{th}$ *IEEE International Conference on Information, Communications and Signal Processing*, 2007, pp. 1–5.

[3] K. Bowyer, K. Hollingsworth, and P. Flynn, "Image understanding for iris biometrics: A survey," *Computer Vision and Image Understanding, vol. ??, no. ??*, pp. ??–??, 2008.

[4] American National Standards Institute, "American National Standard for the safe use of lasers and LEDs used in optical fiber transmission systems," 1988, aNSI Z136.2.

[5] Commission International de l'Eclarirage, "Photobiological safety standards for safety standards for lamps," 1999, report of TC 6-38; CIE 134-3-99.

[6] A. Ross, S. Crihalmeanu, L. Hornak, and S. Schuckers, "A centralized web-enabled multimodal biometric database," in *Proceedings of the 2004 Biometric Consortium Conference (BCC)*, U.S.A, September 2004.

[7] H. Proença and L. A. Alexandre, "The NICE.I: Noisy Iris Challenge Evaluation, Part I," in *Proceedings of the IEEE First International Conference on Biometrics: Theory, Applications and Systems (BTAS 2007)*, Washington, September 2007, pp. 27–29.

[8] Y. He, J. Cui, T. Tan, and Y. Wang, "Key techniques and methods for imaging iris in focus," in *Proceedings of the IEEE International Conference on Pattern Recognition*, August 2006, pp. 557–561.

[9] J. G. Daugman, "High confidence visual recognition of persons by a test of statistical independence," *IEEE Transactions on Pattern Analysis and Machine Intelligence, vol. 25, no. 11*, pp. 1148–1161, November 1993.

[10] ——, "How iris recognition works," *IEEE Transactions on Circuits and Systems for Video Technology, vol. 14, no. 1*, pp. 21–30, January 2004.

[11] W. Barret, "Daugman's iris scanning algorithm," 2000, http://www.engr.sjsu.edu/wbarrett/publications/pubs.html.

[12] J. L. Cambier, "Iridian large database performance," Iridian Technologies, TR: 03-02, Tech. Rep., 2007, http://iridiantech.com.

[13] International Biometric Group, "Independent test of iris recognition technology," 2005, http://www.biometricgroup.com/reports.

[14] T. Mansfiel, G. Kelly, D. Chandler, and J. Kane, "Biometric product testing final report, issue 1.0," 2001.

[15] J. G. Daugman, "Phenotypic versus genotypic approaches to face recognition," in *Face Recognition: From Theory to Applications*. Heidelberg: Springer-Verlag, 1998, pp. 108–123.

[16] ——, "Computer vision notes," 2007, http://www.cl.cam.ac.uk/teaching/0708/CompVision/CompVisNotes.pdf.